geologica acta

Multiphase dolomitization in the Jutana Formation (Cambrian), Salt Range (Pakistan): Evidences from field observations, microscopic studies and isotopic analysis

S. Khan[1,2]   **and**   **M.M. Shah**[1*]

[1]Department of Earth Sciences, Quaid-i-Azam University
45320 Islamabad, Pakistan

[2]Geosciences Advanced Research Laboratory (GARL), Geological Survey of Pakistan
Shahzad Town, 1461 Islamabad, Pakistan

*Corresponding author

─┤ A B S T R A C T ├─

Excellent dolomite exposures are observed in the eastern Salt Range (Pakistan), where the Cambrian Jutana Formation consists of two distinct units (*i.e.* oolitic – pisolitic unit and massive dolomite unit). Field observations revealed that the lower, oolitic-pisolitic unit mostly comprises medium to thick bedded, interlayered brown yellowish dolostone containing ooids/pisoids and faunal assemblages, and grey whitish sandstone with distinct depositional sedimentary features (*i.e.* trough-, herringbone- and hummocky-cross bedding). The upper massive dolostone unit consists of thick bedded to massive dolostone. These two units are separated by shale. Petrographic studies identified three dolomite types, which include: fine crystalline dolomite (Dol. I), medium-coarse crystalline dolomite (Dol. II) and fracture associated, coarse crystalline dolomite (Dol. III). Stable isotope studies indicate less depleted $\delta^{18}O$ values for Dol. I (-6.44 to -3.76‰V-PDB), slightly depleted $\delta^{18}O$ values for Dol. II (-7.73 to -5.24‰V-PDB) and more depleted $\delta^{18}O$ values for Dol. III (-7.29 to -7.20‰V-PDB). The $\delta^{13}C$ values of the three dolomite phases are well within the range of Cambrian sea-water signatures. Furthermore, $\delta^{26}Mg$-$\delta^{25}Mg$ signatures (Dol. I; $\delta^{26}Mg$=-1.19 to -1.67, $\delta^{25}Mg$=-0.61 to -0.86 and Dol. II; $\delta^{26}Mg$=-1.34 to -1.59, $\delta^{25}Mg$=-0.70 to -0.83) indicate three phases of dolomitization in different diagenetic settings. First, an initial stage of dolomitization during the early Cambrian resulted from altered marine, Mg-rich fluids associated with mixing zone mechanism. Second, a late stage of dolomitization was associated with burial during late Permian. A third dolomitization phase was related to post-Eocene times.

INTRODUCTION

Dolomite is a carbonate mineral and constitute a major part of dolostone, which is a potential reservoir rock in known giant hydrocarbon fields. Understanding its precipitation and alteration kinetics in present-day conditions remains a complex issue (Warren, 2000). Previous workers presented dolomitization schemes with various diagenetic realms that result from the interaction with fluids of different chemical composition (Dewit *et al.*, 2014, 2012; Martin-Martin *et al.*, 2013; Shah *et al.*, 2012, 2010; Swennen *et al.*, 2012; Nader *et al.*, 2007; Gasparrini *et al.*, 2006; Machel *et al.*, 2004; Nader and Swennen, 2004). In various published case studies, detailed investigations using field characteristics, microscopic observations and isotope analysis (*i.e.* O/C and Mg-) helped in deciphering dolomite formation and associated diagenetic environment (Zhang *et al.*, 2012; Bontognali *et al.*, 2010; Vasconcelos *et al.*, 2005; Machel, 2004; Machel and Lonnee, 2002; Warren, 2000; Budd, 1997; Last, 1990). According to Zenger *et al.* (1980), 50% of the identified hydrocarbon reservoirs in carbonate rocks are associated with dolomites, where Ghawar oil field of Saudi Arabia contains one-eighth of the world's demonstrated reserves (Cantrell *et al.*, 2004). Reservoirs of the Appalachian and Michigan basins of North America are also associated with dolomites (Keith, 1989).

The study area forms part of the eastern Salt Range, where Jutana Formation (Cambrian) exhibits excellent exposures in various N-S oriented gorges (Fig. 1). Maximum thickness (*i.e.* 84.5m) of the studied Jutana Formation is attained at the type locality near Jutana village (expressed as "G" in Fig. 1) (Shah, 2009). The underlying Kussak Formation (lower Cambrian) and the overlying Baghanwala Formation (upper Cambrian) exhibit normal contact with the Jutana Formation respectively (Shah, 2009). In the adjoining Potwar Basin, the Jutana Formation is a proven hydrocarbon reservoir which consists dominantly of dolostone (80%) and sandstone (20%) (Wandrey *et al.*, 2004; Fig. 1). In order to better constrain the reservoir properties, the present study focuses on the study of the diagenetic evolution of the dolostone sequence of the Jutana Formation. Two selected outcrop sections were identified and sampled (*i.e.* Khewra gorge and exposures along M-2 motorway, eastern Salt Range, Pakistan; Fig. 1). The studied succession consists of three units (*i.e.* interbedded dolostone-sandstone unit and massive dolostone unit), separated by a shale interval (Shah, 2009). The existence of facies variations and more porous dolomitic intervals within the formation demonstrates its excellent hydrocarbon reservoir properties in the area (Ahmad *et al.*, 2013; Quadri and Quadri, 1996; Kadri, 1995).

The porosity and permeability of a carbonate reservoir is affected by diagenetic modifications, which are mainly controlled by the chemical characteristics of the host rock and pore fluids, the flow rate of fluids and the depositional history of the area (Zenger *et al.*, 1980). In the present study, a detailed paragenetic sequence of various diagenetic phases has been established based on field studies and petrographic observations. In addition, the dolomitization mechanisms are proposed in line with conceptual dolomitization models to further explain and constrain the main impact of diagenesis in reservoir rocks.

TECTONO-SEDIMENTARY SETTINGS

During Cambrian times, the study area (part of the Gondwanaland) experienced warm, shallow marine conditions (Kazmi and Jan, 1997; Kadri, 1995). Deposition of clastics, evaporites and limestones took place in lagoonal and shallow marine environments (Kadri, 1995). The study area being part of the Indian plate experienced diverse climatic changes due to plate latitudinal drift from Jurassic to Miocene times. According to Chatterjee *et al.*, 2013, the Indian plate was part of the super continent Gondwanaland, where Australia and Antarctica were situated adjacently. During early Jurassic, complete detachment of Pangea resulted in the formation of eastern and western Gondwanaland respectively, followed by northward drift of the Indian plate after detachment from Australia and Antarctica during the early Cretaceous (Chatterjee *et al.*, 2013). In the early Cretaceous, the Indian plate collided with Kohistan-Ladakh Island Arc (KIA), followed by continental collision of the Indian and Eurasian plates during the early Eocene (Allègre *et al.*, 1984; Molnar and Tapponnier, 1977). Continued collision of the Indo-Eurasian plates resulted in the Himalayan orogeny. Regional thrust systems developed which included the Main Karakoram Thrust (MKT, Eurasia-KIA), the Main Mantle Thrust (MMT, India-KIA), the Main Boundary Thrust (MBT) and the Salt Range Thrust (SRT), bringing older sedimentary successions on top of younger rocks (Malinconico, 1989; Gansser, 1981, 1964; Seeber and Armbruster, 1979; Fig. 1).

The study area is part of the Salt Range, where the SRT acted as a regional decollement for Paleozoic successions thrusted over Neogene sediments of the Jhelum Plain in Pleistocene times (Kazmi and Jan, 1997; Lillie *et al.*, 1987; Yeats *et al.*, 1984; Gee, 1945). The stratigraphic record of the Salt Range exhibits sedimentary successions from Pre-Cambrian to recent times, with the occurrence of few regional and local unconformities (Fig. 2). The studied succession (Jutana Formation) is part of the Jhelum Group, which comprises sandstone, shale and dolomite forming distinctive sedimentary cycles (Shah, 2009; Yeats and Hussain, 1987; Noetling, 1901; Fleming, 1853). The lower
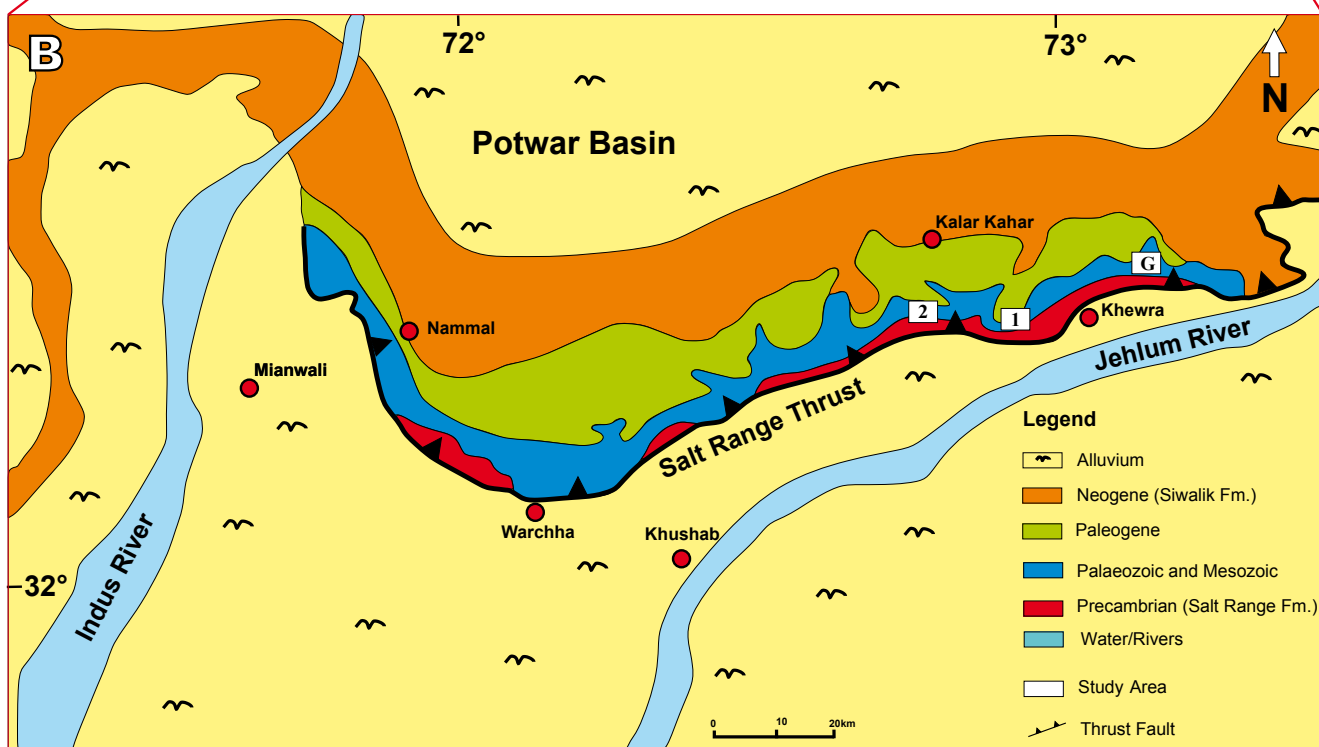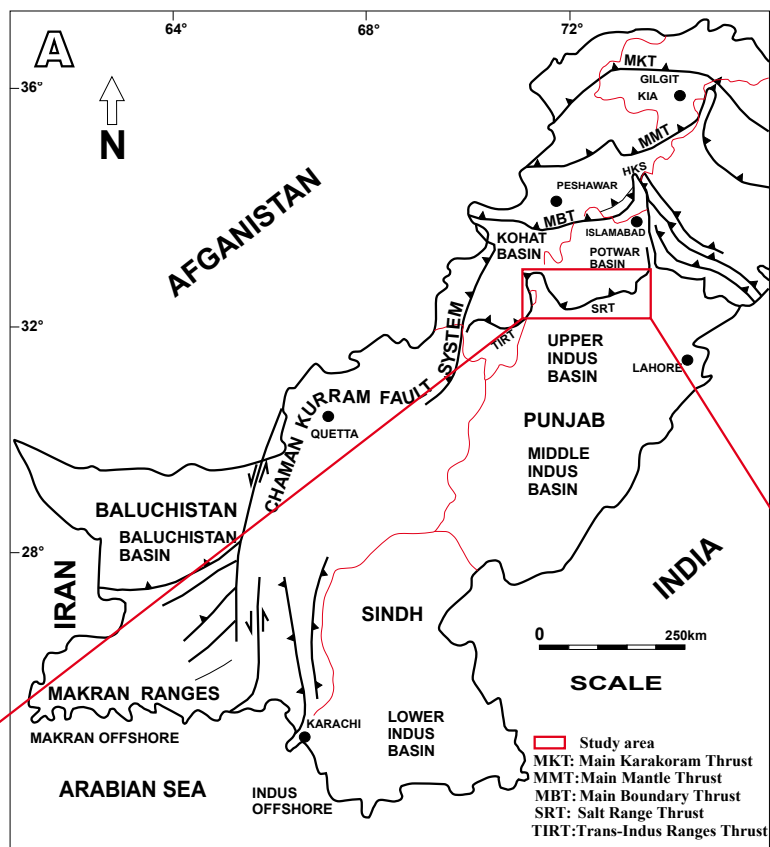
FIGURE 1. A) Tectonic map of Pakistan showing the location of Salt Range (red box). B) Enlargement shows the geological map of Salt Range, where Paleozoic rocks are thrusted over Quaternary alluvial deposits along Salt Range Thrust. White squares indicate location of studied areas; 1: Khewra gorge section; 2: Motorway section, G: Jutana village.

part of the Jutana Fm. comprises interbedded sandstone and dolostone lithologies that resulted from cyclic deposition of clastic and non-clastic sediments. Clastic sediments contain well-preserved depositional sedimentary structures (*i.e.* ripple marks, trough and herring-bone cross-bedding) and demonstrates a transition from sub-tidal to intertidal depositional settings (Ahmad *et al*., 2013; Ghauri, 1979;

Khan, 1977). The upper part of the Jutana Fm. consists of massively bedded, yellow dolomite and cross-bedded (herringbone) sandstones, suggesting intertidal to supratidal depositional conditions before diagenetic modifications. The formation has its lower and upper conformable contact with the Kussak Formation (shale, greenish grey glauconitic micaceous sandstone, interbedded light grey
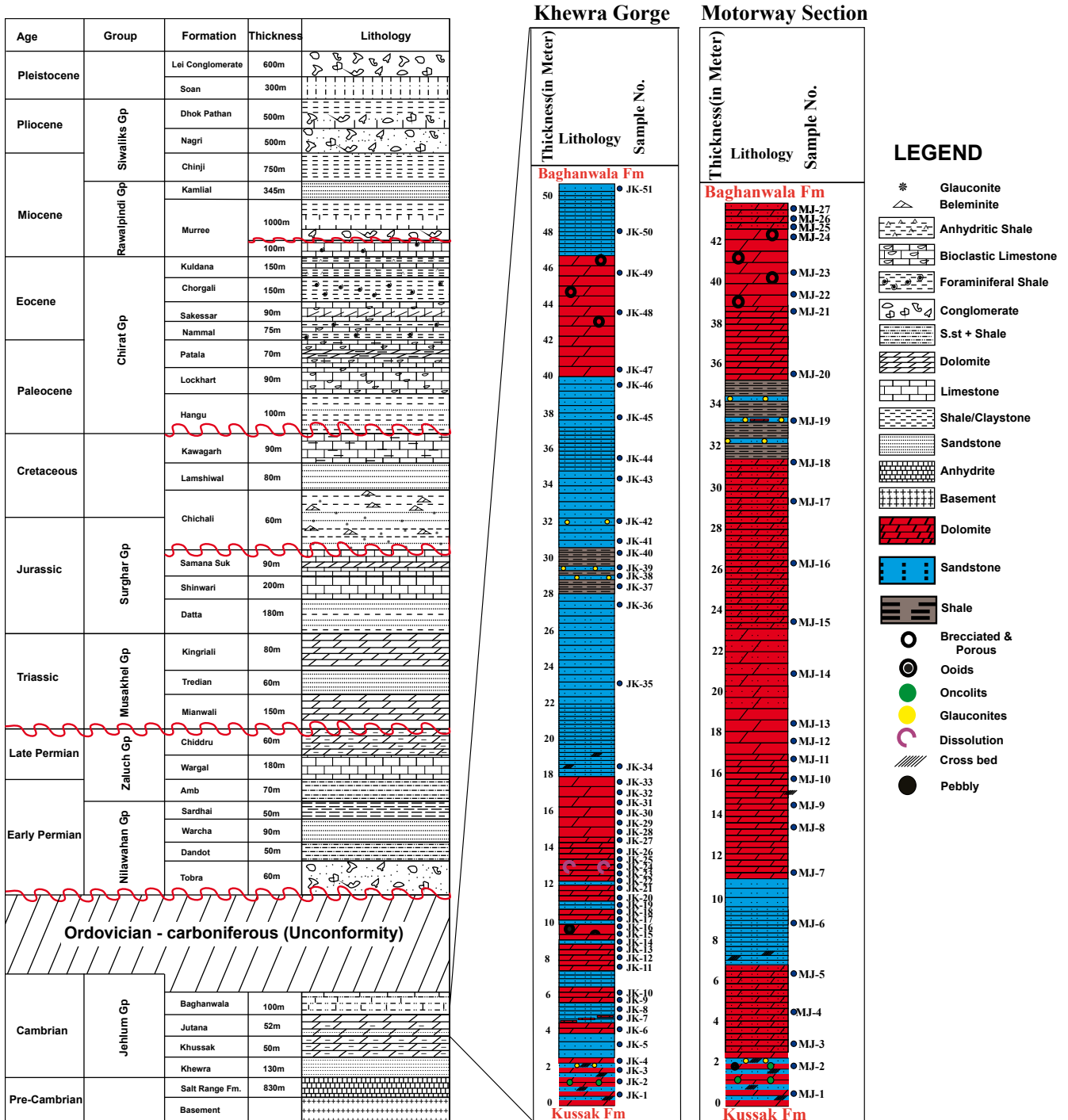

FIGURE 2. Lithostratigraphic chart of the Salt Range. Red undulating lines indicate unconformities (Modified after Shah, 2009). Inset columns show stratigraphic logs of two sampled sections (*i.e.* Khewra gorge and Motorway) of the Jutana Formation.

dolomite) and Baghanwala Formation (red shale and clay with alternate beds of flaggy sandstone and cast of salt pseudomorphs) respectively, both of Cambrian age (Shah, 2009).

METHODOLOGY

Field observations at the two studied sections (*i.e.* Khewra gorge section and Motorway section; Fig. 1) helped to identify various depositional as well as diagenetic features. Selected representative samples from both sections were examined macroscopically. In total, 183 thin sections were prepared in the thin section laboratory of Geoscience Advance Research Laboratories, Geological Survey of Pakistan, Islamabad. The thin sections were studied using polarizing microscope (Olympus CX41) with digital camera fitted (Olympus DP21) for dolomite phase identification and subsequent diagenetic environment determination. 62 stable isotopes ($\delta^{13}C$ and $\delta^{18}O$) analyses were performed at Pakistan Institute of Nuclear Science and Technology (PINSTECH), Islamabad. Oxygen and carbon stable isotopic composition of dolomite phases was analyzed. Sampling was performed with a micro drill equipped with 0.4 to 1mm diameter bits. Powdered dolomite preparations were reacted with phosphoric acid for 3 and 15min respectively in vacuum at standard temperature and pressure conditions. The evolved CO_2 was analyzed on a Thermo Finnigan MAT-252 mass spectrometer. Results were corrected and expressed in relation to the standard Vienna Pee Dee Belemnite (VPDB), reporting a precision of ±0.02 for $\delta^{13}C$ V-PDB and of ±0.04 for $\delta^{18}O$ V-PDB. In addition, 4 samples were analyzed for Mg isotopes ($\delta^{25}Mg$ and $\delta^{26}Mg$) at the Institute of Geology, Mineralogy and Geophysics, Ruhr-University Bochum, Germany. The solution was dried and re-dissolved with 250μl of a 1:1 mixture of HNO_3 (65 %) H_2O_2 (31 %). Subsequently, the solution was evaporated and again re-dissolved in 1.25M HCl. According to Immenhauser *et al.* (2010), Mg-bearing fraction was extracted by using ion-exchange columns (Bio-Rad ion exchange resin AG50 W-X12, 200 to 400 mesh), evaporated to dryness and a 500ppb Mg-solution (in 3.5% HNO_3) was prepared. The samples were analyzed with Thermo Fisher Scientific Neptune MC-ICP-MS using DSM3 standard solution. The external precision was determined by measuring the mono-elemental solution Cambridge 1 against DSM3 standard solution repeatedly (n=4, $\delta^{25}Mg$:-0.75±0.02‰ 2σ and $\delta^{26}Mg$:-1.44±0.05‰ 2σ).

## RESULTS

Field observations

Total thickness of the Jutana Fm. in the Khewra gorge and the Motorway sections is 52m and 43.7m, respectively, where Jutana Fm. consists of three distinct units (Fig. 3A, B). These include: i) Alternating sandstone and dolomite unit; ii) Middle shale unit and iii) Massive dolostone unit.

The lower unit (the sandstone/dolostone unit) has a thickness of 31m and 28m in the Khewra gorge and motorway sections, respectively. In the Khewra gorge section, this unit represents medium to thick bedded light cream to grey color dolomites with alternating layers of medium to thinly laminated impure micaceous sandstone (Fig. 4A-C). Well preserved primary sedimentary structures (*i.e.* cross-bedding and ripple marks) are typically associated with sandstone successions (Fig. 4B-C). In addition, dolomite beds contain foraminiferal assemblages and centimeter scale ooids and pisolites (Fig.
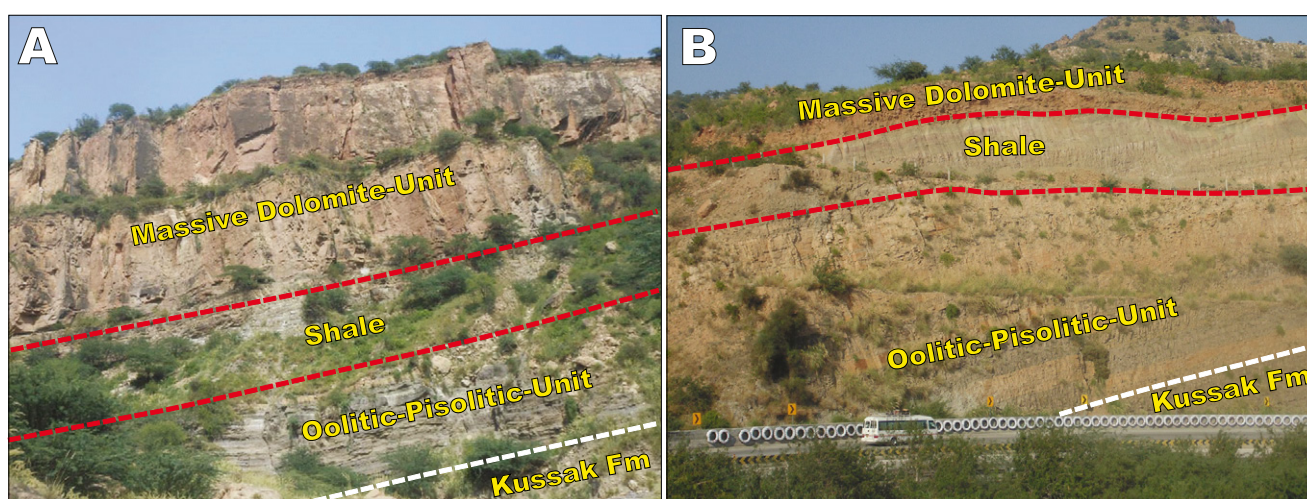
FIGURE 3. Field photographs of Jutana Formation (Fm.) in the eastern Salt Range: A) stratigraphic units of Jutana Fm. in the Khewra gorge section and B) main units of Jutana Fm. in the Motorway section. The contact of Jutana Fm. with the underlying Kussak Fm. is shown in both locations.
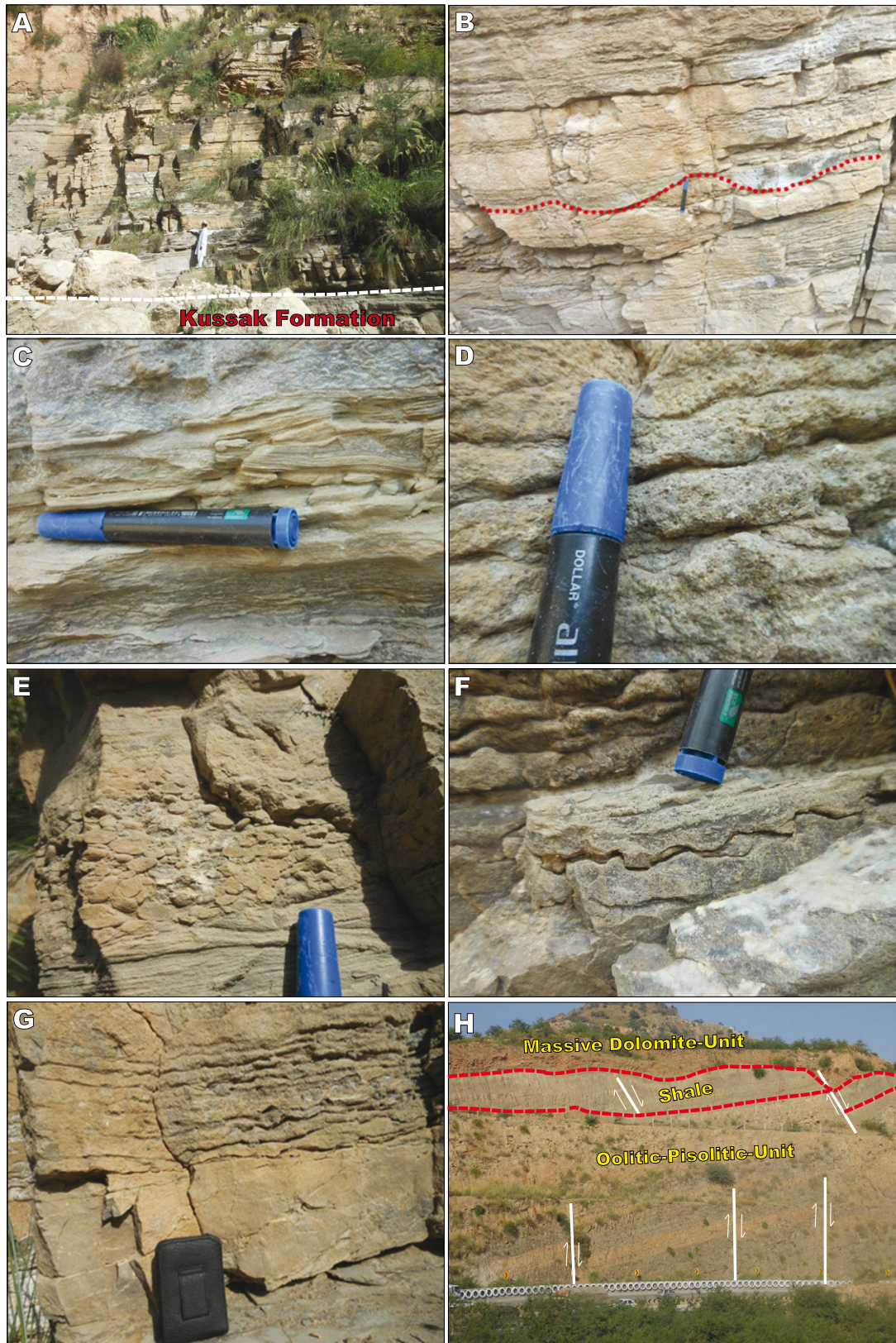
FIGURE 4. Detailed field characteristics of the Jutana Formation: A) Contact between the shales of the Kussak Formation and thin to medium, interbedded sandstones and dolostone; B) Centimeter-scale ripple marks in the sandstone beds; C) Low-angle, cross bedded sandstones; D) Dolomitized limestone with preserved foraminiferal assemblages,; E) Oolitic pisolitic unit in the dolomitized part; F) Bedding parallel stylolites; G) Fractures development in the studied dolostone and H) Panoramic view of the Motorway section, showing normal faulting.

4D, E). Oolitic and pisolitic beds alternating with cross-bedded sandstones, exhibit boudinage that resulted from early deformation due to overburden pressure (Fig. 4E). Bedding parallel stylolites and intensive fracturing are also found in this unit (Fig. 4F-G). In the Motorway section, excellent exposures consist of interbedded dolostone and sandstone (Fig. 4H). Oolitic-pisolitic units are frequent in the dolomitic beds. Tectonic features include faulting that resulted in step-like geometry (Fig. 4H).
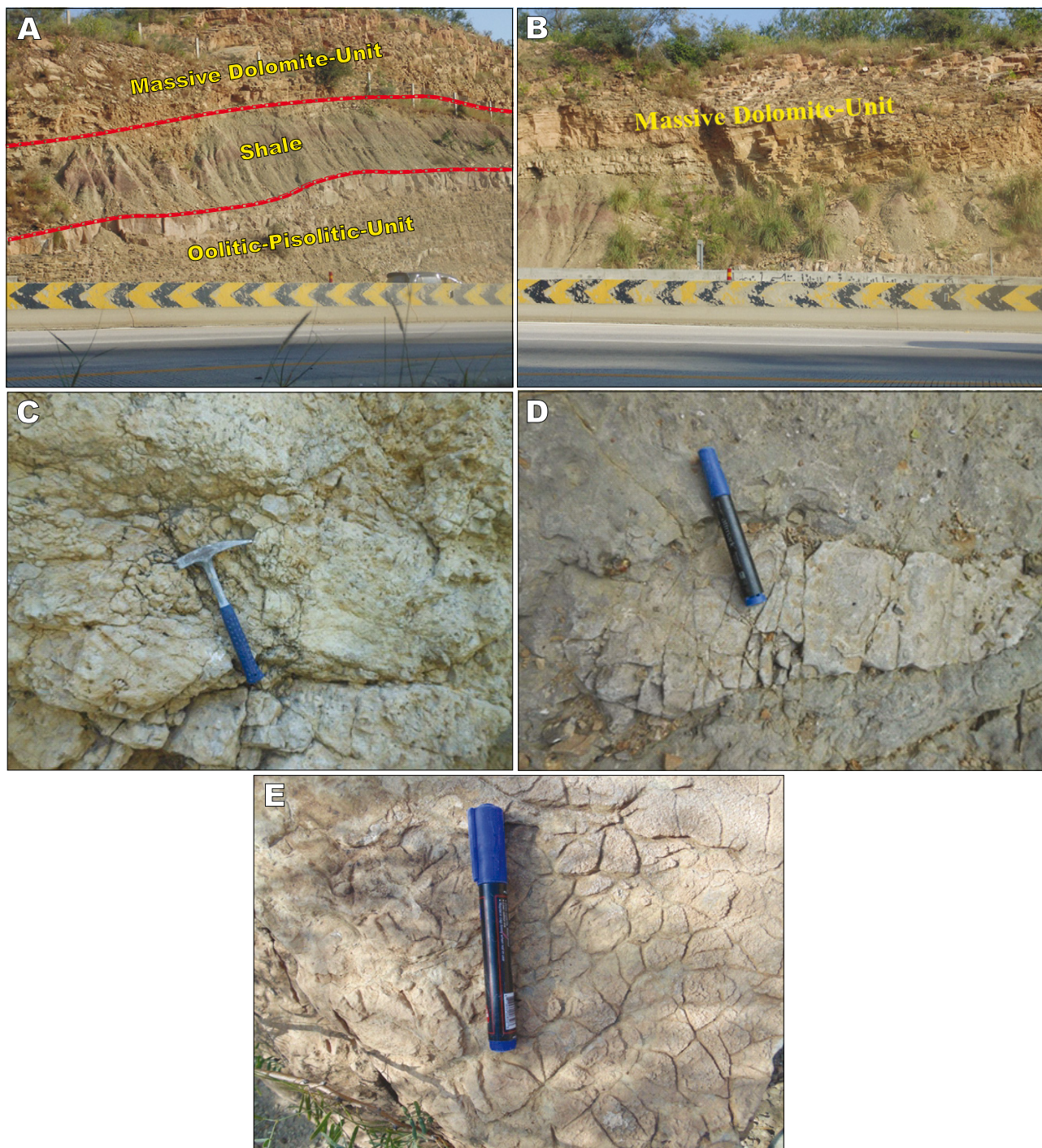
FIGURE 5. Field observations of Jutana Formation: A) Along the road cut side of M-2 Motorway, the three main subdivisions of Jutana Formation are well exposed with the lower part representing the oolitic-pisolitic unit, followed by the shale unit that is overlain by the massive dolomitic unit; B) M-2 Motorway section, upper massive unit is exposed consisting of dolomite; C) Highly fractured massive dolomitic unit in the M-2 Motorway section; D) Isolated clast of host limestone embedded in dark grey colored dolomite and E) Distinct chop-board weathering observed in the massive dolomite unit of Khewra section.

The middle shale unit is dark-grey greenish to maroon shale, interbedded with glauconitic sandstone (Fig. 5A, B). Its thickness varies from 3 to 4 meters in the studied sections (Fig. 5A). Various fossils (*i.e. Linguelella fuchsi, Botsfordia, Reedlichia noetlingi* and a gastropod identified as *Pseudotheca* ef. *Subrugosa*) have been reported (Teichert, 1964). This unit exhibits similarities to the underlying Kussak Formation.

The upper massive dolostone unit in the Khewra gorge section is composed of massive to thick-bedded yellow dolomite (~31m thickness), exhibiting intense fracture density (Fig. 5C). It is highly deformed, shows chop-board weathering (Fig. 5C-E), and contains isolated clast of host limestone embedded in dark grey colored dolomite (Fig. 5D). In the Motorway section, similar features as in the Khewra gorge section are observed.

Petrography

Thin sections of precursor limestone (partially dolomitized) showed distinct depositional features that include ooids, pisolites, intraclasts, foraminiferal assemblages, and relics of various unidentified fossils. Partially altered limestone contain ooids with concentric rims, whereas similar ooids are completely dolomitized in other parts of the studied sections (Fig. 6A-B). It is noteworthy that the upper part of the Jutana Formation shows relics of precursor limestone, whereas the lower part is completely dolomitized. In the next section, the various dolomite phases are discussed in order to understand the diagenetic processes that affected the studied rocks, which include: i) fine crystalline, euhedral dolomite matrix (Dol. I) that form the major part of the dolomitized Jutana Formation, followed by ii) medium to coarse crystalline, anhedral dolomite (Dol. II) mostly observed in replaced ooids and pisolites (Fig. 6C-F) and iii) coarse crystalline, anhedral dolomite cement (Dol. III) exhibiting fracture-filling and saddle type dolomite cement (Figs. 6D; 7A-B).

Fine crystalline matrix dolomite (Dol. I)

In the Khewra gorge section, microcrystalline to fine crystalline dolomite (Dol. I) is of light grey color (Fig. 6C). Such replacive dolomite exhibits crystal size <10μm, displays nonplanar-a to planar-s texture with irregular intercrystalline boundaries, and is characterised by the fabric preservation of the precursor lithology (Fig. 6C-D), containing partially altered ooids and peloids respectively (Fig. 6D). In addition, vuggy and moldic porosity form part of such dolomite in the Khewra gorge section (Fig. 6B, D).

In the Motorway section, Dol. I is characterised by matrix associated finely crystalline dolomite (Fig. 6E, F). The dolomite crystals are relatively closely packed,

equigranular, euhedral to subhedral. Dol. I mostly occurs around oolitic and peloidal grains, which are completely replaced by medium to coarse crystalline dolomite (Dol. II; Fig. 6E, F). In addition, Fe- rich residue (*i.e.* pyrite) mostly occurs along the crystal boundaries in all observed dolomite types (Fig. 6D).

### Medium-coarse crystalline dolomite (Dol. II)

In the Khewra gorge section, brown, medium to coarse crystalline planar-s to planar-e type dolomite (Dol. II) mostly occurs as replacive dolomite (Sibley and Gregg, 1987). The crystal size of such dolomite ranges from 90 to 200μm, and is characterized by its fabric destructive character and local preservation of the precursor's texture (Fig. 6D). It is noticeable the presence of pores and relics of various fossil fragments (Fig. 6D). Other associated features include; fabric destructive fractures and seams of stylolites, where dark pyrite occur along stylolite seams (Fig. 7A). Petrographic studies and scanning electron microscopy also shows pyrite crystals engulfed in glauconite grains (Fig. 7B, C). In general, porosity is negligible, but fracture-associated porosity is observable in Dol. II (Fig. 7E).

According to Sibley and Gregg (1987), Dol. II are planar/idiotopic-e to planar/idiotopic-s in the Motorway section. In this section, replacive dolomite (Dol. II) mostly occurs in replaced ooids (Fig. 6E), where the abundance of the replaced ooids is high compared to Khewra gorge section (Fig. 6E, F). Some unidentified skeletal fragments and burrows are also present (Fig. 6E). Dol. II displays scattered rounded pale-green glauconitic grains (Figs. 6E; 7B). Dol. II is locally highly fractured, and the fractures are filled with calcite cement (Figs. 7B). In addition, the presence of iron leaching along fractures has been observed (Fig. 6D).

### Coarse crystalline fracture filling dolomite (Dol. III)

This phase shows the presence of coarse crystalline, fracture filling dolomite cement (Dol. III; Fig. 7D, E). Crystal size varies from 200μm up to 3mm with planar-nonplanar and euhedral to subhedral textural characteristics. Dol. III mostly occurs along fracture openings, in the form of coated cement around Dol. I and Dol. II crystals (Fig. 7D). The growth of dolomite is clear along fractures showing multiple growth rims (Fig. 7D). In the studied samples, the residual space after Dol. III cement precipitation is filled by calcite cement (Fig. 7D). Likewise, samples from the Motorway section exhibits dolomite cements of equant, planar to nonplanar and euhedral to subhedral crystals (Fig. 7E). In contrast, samples from the Khewra gorge section have dolomite cement rims of Dol. III relatively thicker than dolomite rims exhibited in the Motorway section (Fig. 7E).
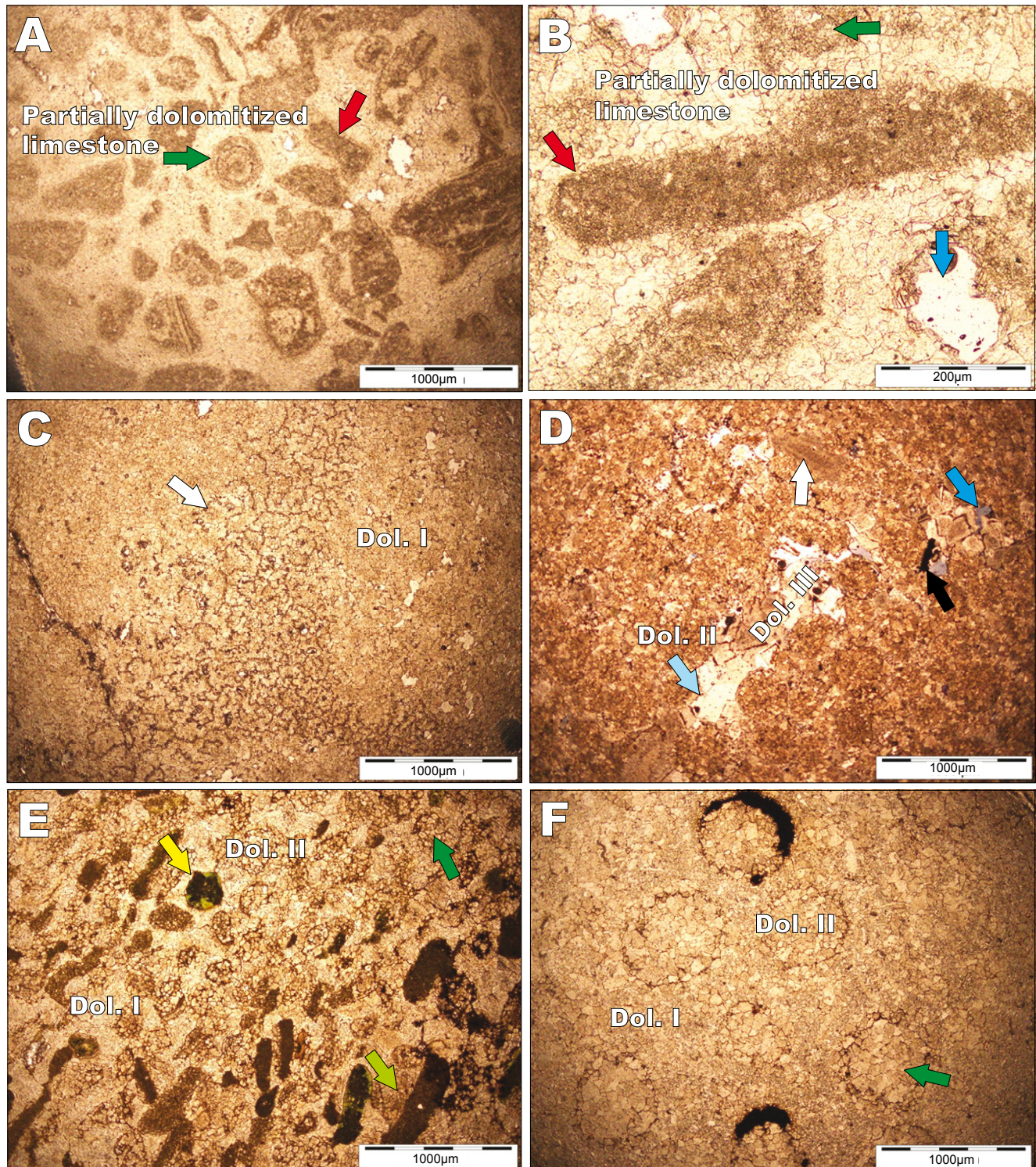
FIGURE 6. Petrographic characteristics of the studied Jutana Formation (Photomicrographs, Plane-Polarized Light, PPL): A) Partially dolomitized limestone with intraclasts (red arrow) and ooids (green arrow); B) Close up of a partially dolomitized intraclast (red arrow) surrounded by off-white colored, coarse crystalline dolomite cement. Note ooid (green arrow) and vuggy porosity (blue arrow); C) Fine to medium crystalline dolomite (Dol. I) containing well preserved algae (white arrow); D) Medium to coarse crystalline dolomite (Dol. II) containing fracture-filled, coarse crystalline dolomite cement (Dol. III), pyrite observed in the fracture-fillings (black arrow), skeletal fragments (white arrow). D) Points fracture porosity (dark blue arrow) and cement (light blue arrow); E) Fine crystalline dolomite (Dol. I) containing oolite (green arrow) filled with medium-coarse crystalline dolomite (Dol. II), glauconite (yellow arrow) and intraclast (light green arrow) and F) Fine crystalline dolomite (Dol. I) and medium-coarse crystalline dolomite (Dol. II) with ooid (green arrow) modified to coarse crystalline dolomite. Both E and F contain ooids of different sizes.
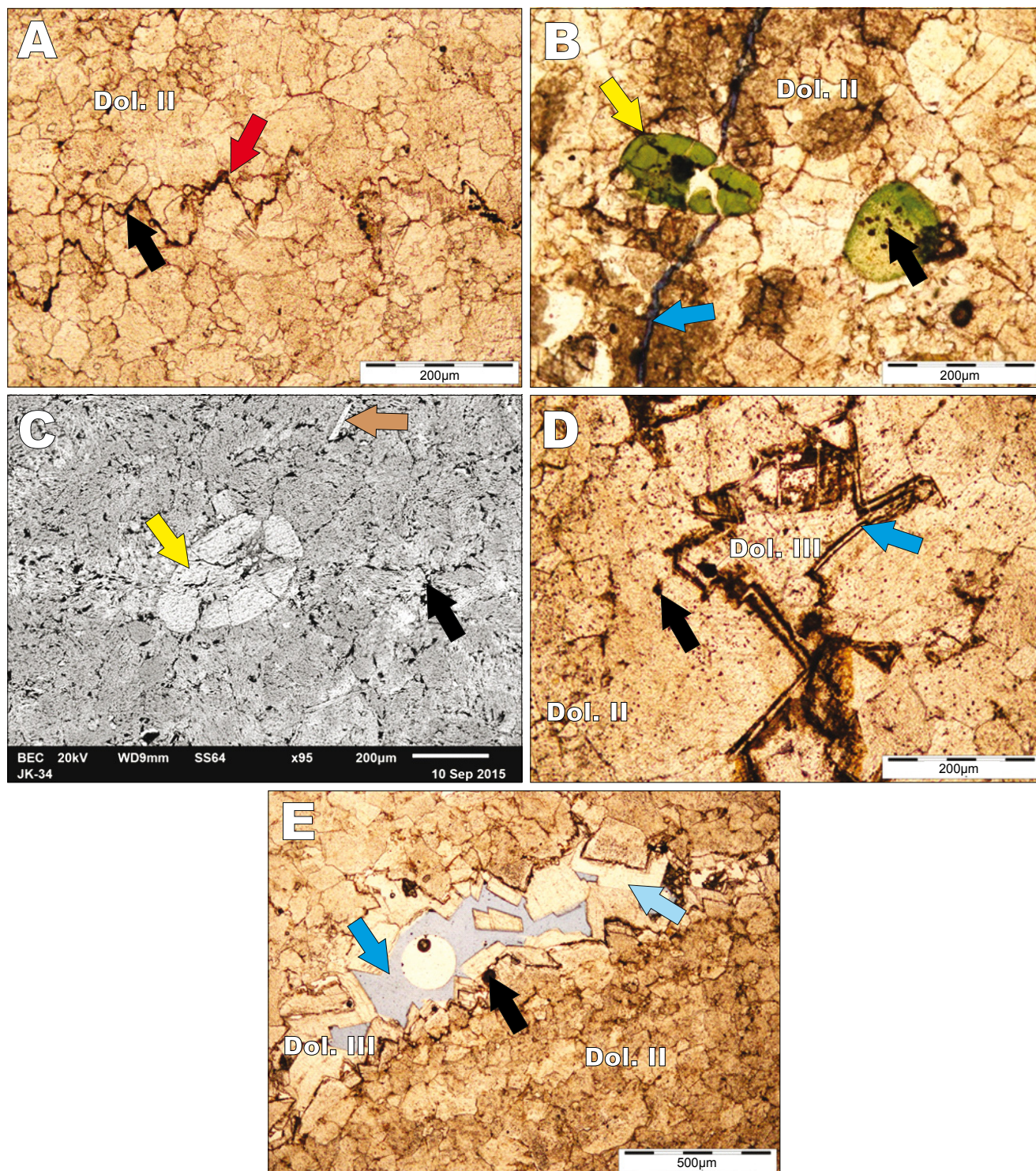
FIGURE 7. Photomicrographs showing the petrographic characteristics of the Jutana Formation. A) Pressure dissolution stylolite (red arrow) in medium-coarse crystalline dolomite (Dol. II) and pyrite (black arrow) along stylolites; B) Green glauconite (yellow arrow) in dolomite and pyrite clasts within fractured glauconite (black arrow), fracture porosity is evident as open fractures (blue arrow); C) Back scattered SEM image, glowing white glauconite (yellow arrow) embedded in light grey colored medium to coarse dolomite (Dol. II), black arrow indicate Fe-residue, lathe shaped mica (brown arrow). D) Medium to coarse crystalline dolomite contains fracture filling, coarse crystalline dolomite (Dol. III) with dark colored crystal boundary (blue arrow), sparse distribution of pyrite is indicated by black arrow; E) Crystal growth cementation in coarse crystalline fracture filling dolomite (Dol. III), whereas porosity reduction (dark blue arrow) is evident due to calcite cementation (light blue arrow), pyrite is distributed along the fractures (black arrow).

Similarly, Dol. III is mostly associated with fractures and openings in the earlier formed dolomite matrix (*i.e.* Dol. I and Dol. II) (Fig. 7E). Besides dolomitization, other features include the presence of rounded, sparsely distributed pale-green colored glauconite (Figs. 6E; 7B, D-E). In addition, accessory heavy minerals are also observed (Fig. 7E). Lastly, fracture porosity is partly filled by calcite cement, which mark the end of diagenetic history of the studied rocks (Fig. 7E).

Isotope analyses

Based on stable isotopes (*i.e.* δ^{18}O and δ^{13}C), deviation from marine signatures indicate diagenetic imprints on the studied rocks. According to Prokoph *et al.* (2008) and Veizer *et al.* (1999), Cambrian marine signatures ranged from -1.00 to 0.00‰V-PDB (δ^{18}O), whereas δ^{13}C signatures tend to range from -2.00 to 0.00‰V-PDB. In the studied sites, the different dolomite phases exhibited a wide range of isotopic signatures (Fig. 8; Table 1). These include Dol. I (δ^{18}O=-6.44 to -3.76‰V-PDB; δ^{13}C=-0.54 to +0.35), Dol. II (δ^{18}O=-7.73 to -5.24‰V-PDB; δ^{13}C= 0.09 to -1.83), and Dol. III (δ^{18}O=-7.29 and -7.20‰V-PDB; δ^{13}C=-1.83 and -1.83). Stable isotope signatures indicate slightly depleted δ^{18}O and δ^{13}C values compared to Cambrian marine environments.

Mg-isotope signatures are important for systematic investigations of various types of diagenetic dolomites formed from different settings and time intervals worldwide (Geske *et al.*, 2014). In four representative samples from the studied sections, δ^{26}Mg ranges from -1.19 to -1.67‰ in Dol. I, and from -1.34 to -1.59‰ in Dol. II, while δ^{25}Mg ranges from -0.61 to -0.86 in Dol. I, and from -0.70 to -0.83‰ in Dol. II (Fig. 9; Table 1).

DISCUSSION

Timing of Dolomitization

The two studied locations of the Jutana Formation (*i.e.* Khewra gorge and Motorway sections) show alternating sandstone and dolostone beds, which contain preserved primary features (*i.e.* ooids and foraminifera, ripple marks and cross-bedding). Petrographic studies distinguished three dolomite phases in the studied rocks (*i.e.* Dol. I, Dol. II and Dol. III (Figs. 6; 7). The presence of glauconite indicates restricted marine condition under low sediment supply conditions (Amorosi, 1997; Odin and matter, 1981; McRae, 1972). Constraints on the relative timing of dolomitization were fundamented on a number of observations. It is observed that an initial phase of partial dolomitization affected the host limestone in the earliest stage of diagenesis. The matrix of the limestone underwent
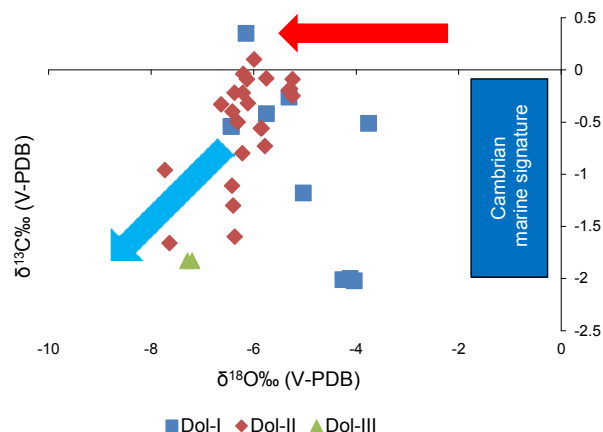
FIGURE 8. Stable isotopes (C and O) signatures of samples from the Khewra gorge and Motorway sections (see the sections in Fig. 2). These isotopic signatures indicate depletion of δ^{18}O compared to Cambrian marine limestones (red arrow), whereas δ^{13}C signatures of the studied dolomite phases are within the range of precursor limestone (blue arrow).

TABLE 1. O/C and Mg isotopes results of selected samples from the studied sections

| Site	Sample	Phase	δ^{18}O	δ^{13}C	δ^{25}Mg	δ^{26}Mg
Khewra	JK-32	Dol-I	-5.75	-0.42		
	JK-33	Dol-I	-5.31	-0.26		
	JK-47	Dol-I	-6.15	0.35		
	JK-48	Dol-I	-5.9	0.13		
	JK-49	Dol-I	-6.44	-0.54	-0.86	-1.67
	JK-50	Dol-I	-6.44	-0.54		
	JK-2a	Dol-II	-6.368	-1.60		
	JK-3	Dol-II	-6.4	-1.3		
	JK-4a	Dol-II	-7.64	-1.66		
	JK-6a	Dol-II	-6.42	-1.11		
	JK-9	Dol-II	-5.86	-0.56		
	JK-11	Dol-II	-5.78	-0.73	-0.70	-1.34
	JK-12a	Dol-II	-7.73	-0.96		
	JK-13a	Dol-II	-6.22	-0.8		
	JK-15	Dol-II	-5.84	-0.56		
	JK-16a	Dol-II	-5.24	-0.09		
	JK-18	Dol-II	-6.11	-0.32		
	JK-20	Dol-II	-6.63	-0.33	-0.83	-1.59
	JK-21a	Dol-II	-6.37	-0.22		
	JK-22	Dol-II	-5.75	-0.08		
	JK-23a	Dol-II	-6.2	-0.04		
	JK-24	Dol-II	-5.29	-0.18		
	JK-25a	Dol-II	-6.21	-0.22		
	JK-26	Dol-II	-5.99	0.1		
	JK-27	Dol-II	-5.24	-0.25		
	JK-29	Dol-II	-5.31	-0.2		
	JK-30	Dol-II	-5.85	0.8		
	JK-31	Dol-II	-6.13	-0.09		
	JK-05	Dol-III	-7.29	-1.831		
Motorway	MJ-20	Dol-I	-4.04	-2.02		
	MJ-23	Dol-I	-5.03	-1.18		
	MJ-26	Dol-I	-3.76	-0.513		
	MJ-27	Dol-I	-4.26	-3.05		
	MJ-2	Dol-I	-4.12	-2.00	-0.61	-1.19
	MJ-4	Dol-II	-6.41	-0.40		
	MJ-10	Dol-II	-6.31	-0.50		
	MJ-5	Dol-III	-7.20	-1.831		
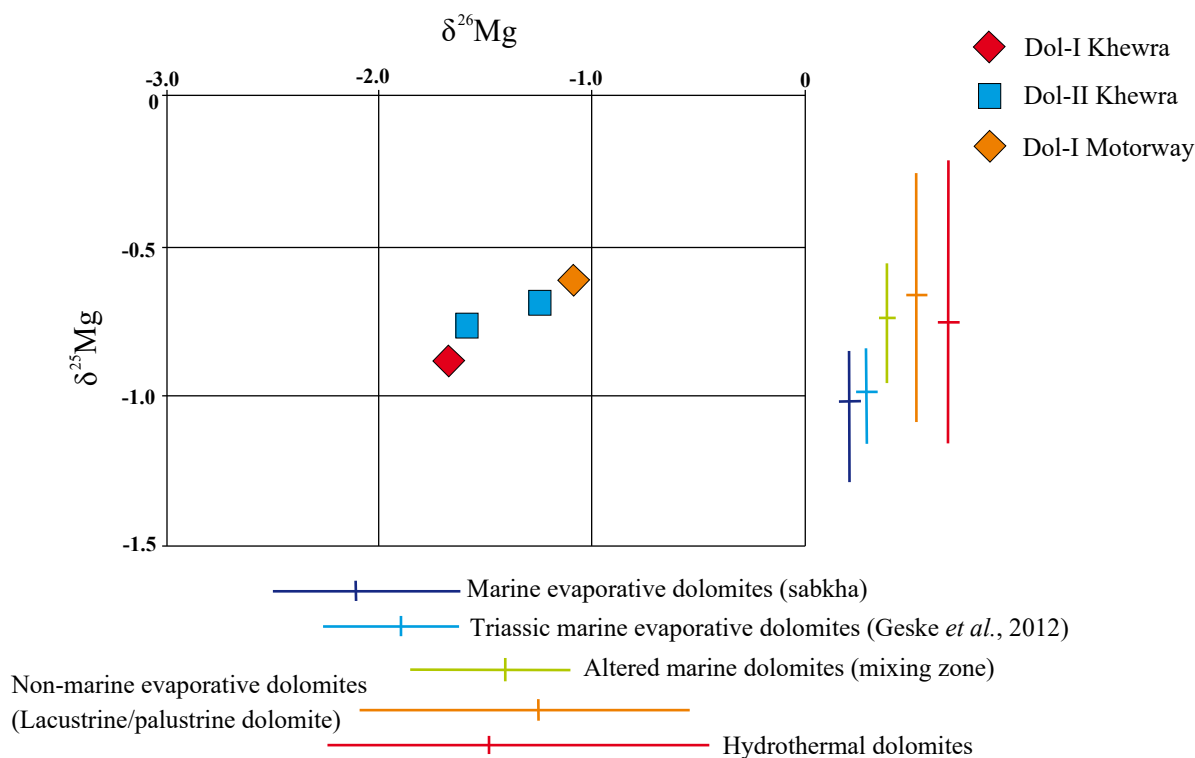
FIGURE 9. Cross plot of Mg-isotopes results (δ^{25}Mg *vs.* δ^{26}Mg) of the studied sections according to Geske *et al.* (2015).

complete dolomitization into Dol. I (Fig. 10A), while ooids and other intraclasts remained unaltered. This argument is supported by three main evidences, which are described as follows. Petrographic observations indicate the presence of quartz grains (average: 8-10%) in the matrix dolomite, which is also confirmed by XRD analysis in another studies (Shah and Khan, accepted). Furthermore, less depleted oxygen isotope signatures (-6.44 to -3.76‰V-PDB) further support Dol. I formation in the earliest stage of diagenesis during the early Cambrian (Fig. 2). As documented in various studies, meteoric diagenesis could have played an active role in the dissolution of ooids during a period of subaerial exposure (Honarmand and Amini, 2012; Mazullo, 1977; Sellwood and Beckett, 1991). Dissolution of unaltered ooids and intraclasts in the partially dolomitized limestone during Ordovician-Carboniferous exposure (Fig. 2) could result from percolating of meteoric fluids, which might have passed through the overlying Baghanwala Formation. During Permian deposition, precipitation of Dol. II in the dissolved ooids is more likely as evidenced by the presence of stylolites post-dating Dol. II (Figs. 7A; 10B). Dol. III represents last stage of dolomitization, where coarse crystalline, saddle type dolomite filled open fractures in Dol. I and II respectively (Figs. 6D; 7D-E). Nonplanar, saddle dolomite exhibits undulose extinction, which is typical of burial conditions (Radke and Mathis, 1980). Such dolomites (*i.e.* Dol. III) formed under tectonic influence (fracture-filling) and burial under ~5000m-thick sedimentary cover, which might be linked to post orogeny

(*i.e.* post Eocene), and before the emplacement of Salt Range Thrust during Pliocene-Pleistocene time (Yeats *et al.*, 1984). Other diagenetic features include the presence of calcite and pyrite, which mark the end of diagenetic history of the studied successions (Figs. 7B-C; 11).

Isotope studies (C, O, Mg) helped constraining dolomitizing fluid chemistry, which lead us to propose possible mechanism of dolomitization (Bowen *et al.*, 2008; Jaffres *et al.*, 2007). O/C isotope signatures indicate less depleted δ^{18}O values for Dol. I, whereas Dol. II and Dol. III represent more depleted δ^{18}O values (Fig. 8). In contrast, reported δ^{13}C values of various dolomite phases are within the range of original marine signatures of the host limestone (*i.e.* Cambrian), thus the carbon isotopic composition of the dolomitizing fluids may have been buffered by the host rock. Mg- isotope signatures further helped in constraining diagenetic conditions. Based on Geske *et al.* (2015), δ^{25}Mg *vs.* δ^{26}Mg crossplot indicates three possible sources of dolomitizing fluids for Dol. I, Dol. II and Dol. III events that include burial activity, non-marine lacustrine or palustrine process and/or altered marine, mixing zone process for dolomitization in the Jutana Formation (Fig. 9).

Mechanism of dolomitization

The studied interbedded carbonate-siliciclastic succession represents tidal flat depositional settings

(Ahmed *et al.*, 2013). The precursor limestone underwent partial dolomitization and resulted in the formation of matrix dolomite Dol. I. As discussed earlier, initial stage of dolomitization occurred during early Cambrian, where restricted, shallow marine conditions prevailed as evidenced by overlying Baghanwala Formation in the study area (Shah, 2009). Furthermore, less depleted $\delta^{18}O$ signatures indicates dolomitization from slightly altered marine waters (Fig. 8). This implies that dolomitization may have resulted from altered marine fluids in the seepage-reflux and/or mixing zone environments during capillary flow through sediments as discussed in various studies (Fu *et al.*, 2006; Jones *et al.*, 2002; Melim and Scholle, 2002; Qing *et al.*, 2001; Al-Aasm, 2000; Müller *et al.*, 1990; Peter and Kinsman, 1981). Furthermore, $\delta^{13}C$ signatures exclude the possibility of seepage reflux conditions of dolomitization, as such conditions are representative of more depleted $\delta^{13}C$ values due to meteoric influx (Machel *et al.*, 1995; Irwin *et al.*, 1977). This is also supported by the absence of evaporites in the studied sites. In brief, mixing zone dolomitization occurred, where Mg-rich fluids of altered marine origin percolated through interbedded sandstone

and limestone successions leading to dolomitization in the platform margin. Pore-filling dolomite Dol. II exhibits more depleted $\delta^{18}O$ values (Fig. 8), hence indicative of dolomitization in the burial regime or changes in $\delta^{18}O$ SMOW of fluids. In addition, fracture-filled, saddle type dolomite Dol. III also indicated highly depleted $\delta^{18}O$ values (Fig. 8) and confirmed burial conditions of its formation.
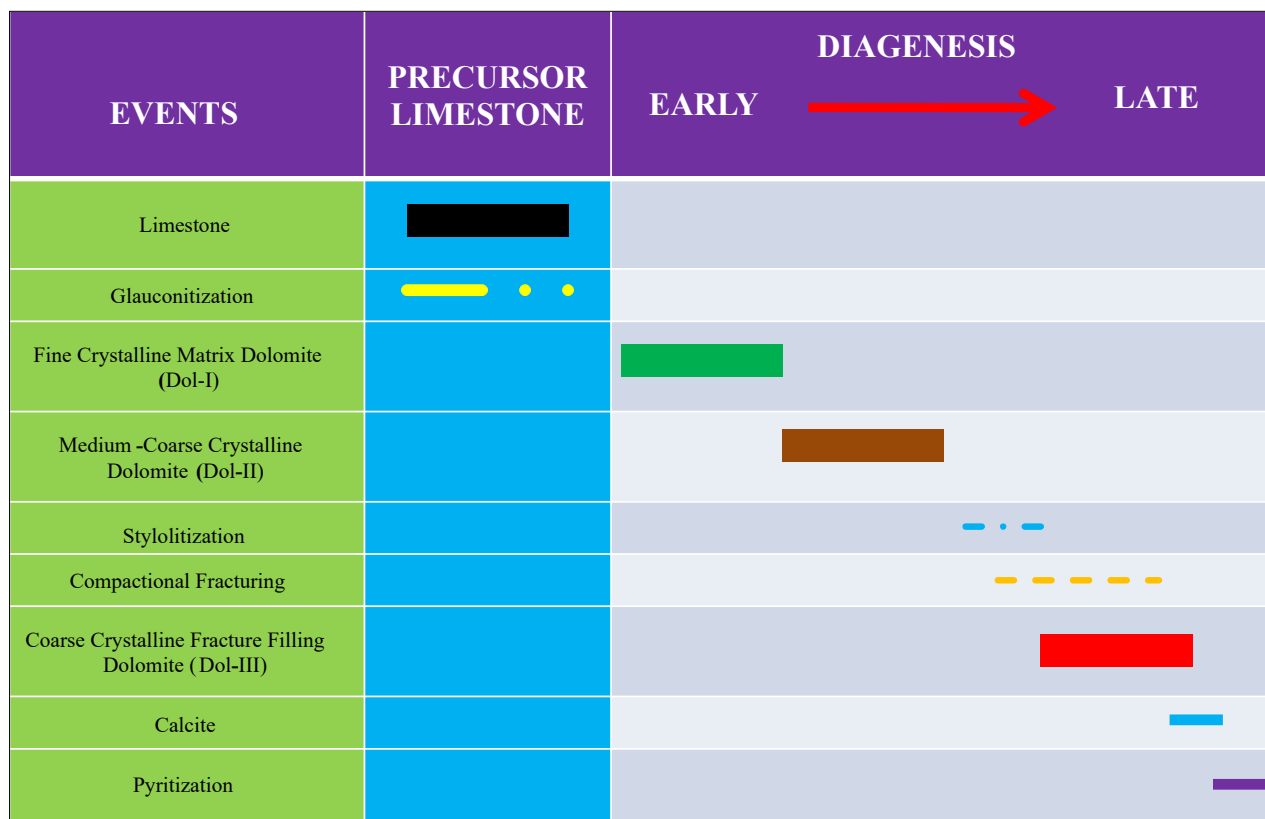
In conclusion, above-mentioned discussion revealed that initial stage dolomites (Dol. I) are compatible with altered marine, mixing-zone related dolomitization fluids, followed by burial associated dolomitization in the form of Dol. II and Dol. III in the study area.

Proposed diagenetic model

Based on the above discussion, it is observed that the interbedded limestone and sandstone of the Jutana Formation underwent dolomitization in the eogenetic, near depositional phase (Fig. 12A). Marine, Mg-rich fluids percolated through interbedded sandstone and limestone, whereas in situ fluids may have
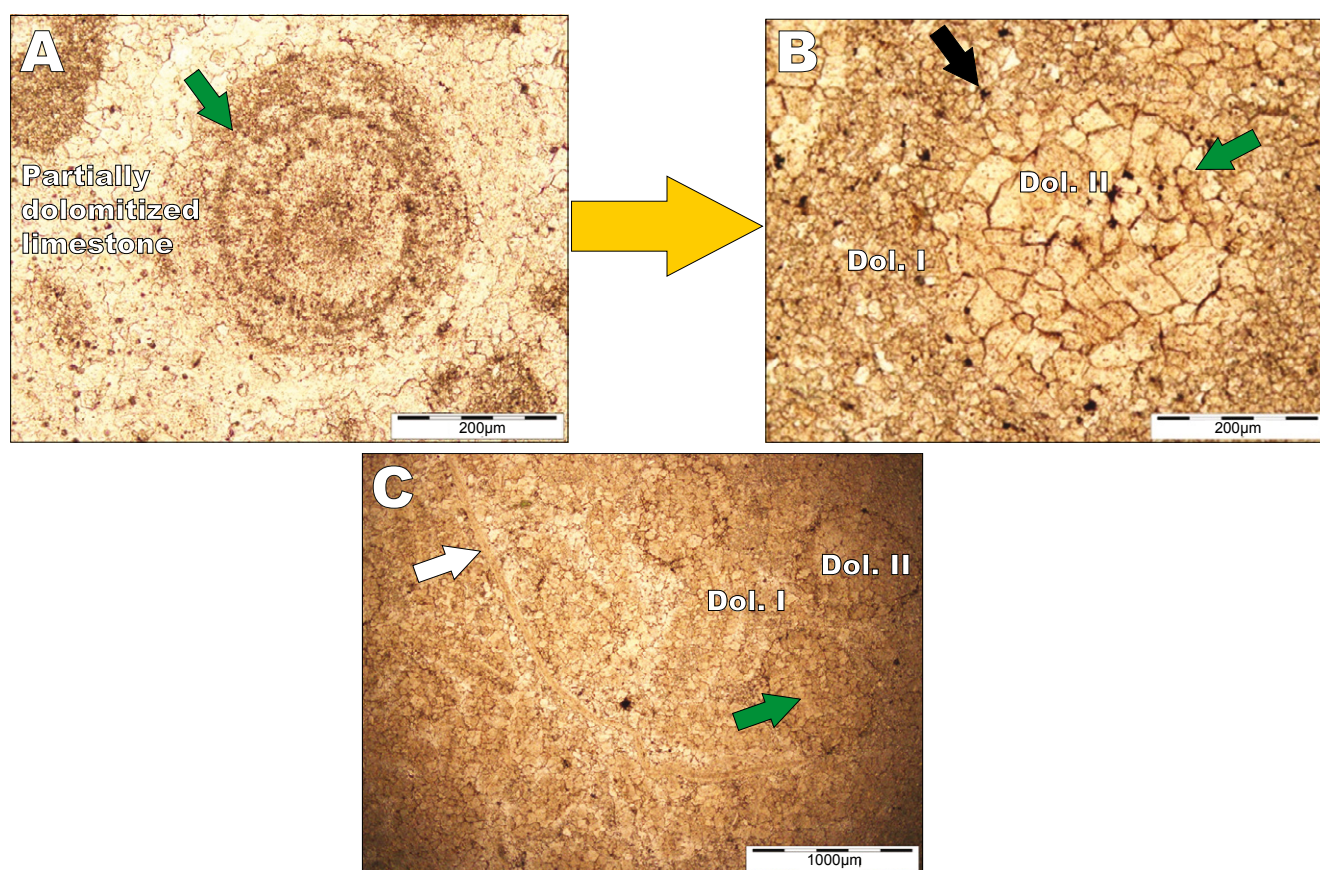
FIGURE 10. Sedimentary facies precursors and diagenetic modifications observed in the studied rocks (Photomicrographs, PPL): A) Partially dolomitized limestone; green arrow: ooid; B) Medium-coarse crystalline dolomite (Dol. II) and fine crystalline dolomite (Dol. I); green arrow: ooid modified to coarse crystalline dolomite, black arrow: iron/heavy mineral residue and C) Fine crystalline dolomite (Dol. I) and medium-coarse crystalline dolomite (Dol. II) with fossil fragments; white arrow: fossil fragment, green arrow: ooid modified to coarse crystalline dolomite.

EVENTS	PRECURSOR LIMESTONE	DIAGENESIS		
		EARLY		LATE
Limestone	▬			
Glauconitization	▬ ● ●			
Fine Crystalline Matrix Dolomite (Dol-I)		▬		
Medium -Coarse Crystalline Dolomite (Dol-II)		▬		
Stylolitization			▬ · ▬	
Compactional Fracturing			▬ ▬ ▬ ▬	
Coarse Crystalline Fracture Filling Dolomite (Dol-III)			▬	
Calcite				▬
Pyritization				▬

FIGURE 11. Detailed paragenetic history of the dolomite of Jutana Formation, representing early diagenetic modifications in the host limestone, followed by middle to late stage diagenetic alterations.

altered marine, Mg-rich fluids, leading to the partial dolomitization of the limestone succession with the formation of matrix dolomite (Dol. I; Fig. 12B). During the Cambro-Ordovician exposure, dissolution of ooids due to meteoric influx occurred in the partially dolomitized limestone (Fig. 12C). This was followed by a second phase of dolomitizing fluids originated from deep-seated sediments due to initial burial activity (based on moderate depleted stable isotope signatures), which resulted in pore-filling of dissolved ooids (Dol. II; Fig. 12D). Post orogenic events caused fracture development in Dol. I and Dol. II (Fig. 12E). In a last stage, fracture-filling type dolomitization (*i.e.* Dol. III) resulted from burial associated fluids of relatively more depleted stable isotope signatures as compared to Dol. II during Eocene-Pleistocene time (Fig. 12F).

CONCLUSIONS

Field observations in the three main units of Jutana Formation (*i.e.* lower oolitic/pisolitic, middle shale and upper massive dolomitic unit) indicate interbedded dolostone-sandstone successions, containing depositional features in the sandstone (*i.e.*

ripple marks, cross-bedding) and precursors of original limestone in dolostone (*i.e.* mica laths, ooids, pisolites, intraclasts, glauconite and foraminiferal assemblages). The presence of glauconite grains represent restricted marine conditions for the formation of the precursor limestone.

Petrographic studies helped in delineating three dolomite phases of distinct characteristic features. These include; Fine to medium crystalline, matrix dolomite (Dol. I), Medium to coarse crystalline, replacive dolomite (Dol. II) and coarse crystalline, fracture-filling dolomite cement (Dol. III) respectively.

O/C isotope analysis; Dol. I (δ^{18}O=-6.44 to -3.76‰V-PDB; δ^{13}C=-0.54 to +0.35), Dol. II (δ^{18}O=-7.73 to -5.24‰V-PDB; δ^{13}C=-0.09 to -1.83) and Dol. III (δ^{18}O=-7.29 and -7.20‰V-PDB; δ^{13}C=-1.83 and -1.83) and Mg-isotope values (*i.e.* Dol. I; δ^{26}Mg=-1.19 to -1.67, δ^{25}Mg=-0.61 to -0.86 and Dol. II; δ^{26}Mg=-1.34 to -1.59, δ^{25}Mg=-0.70 to -0.83) indicate diverse signatures of above mentioned different dolomite types.

Petrographic observations and isotopic signatures (O/C and Mg) indicate multiple phases of dolomitization.
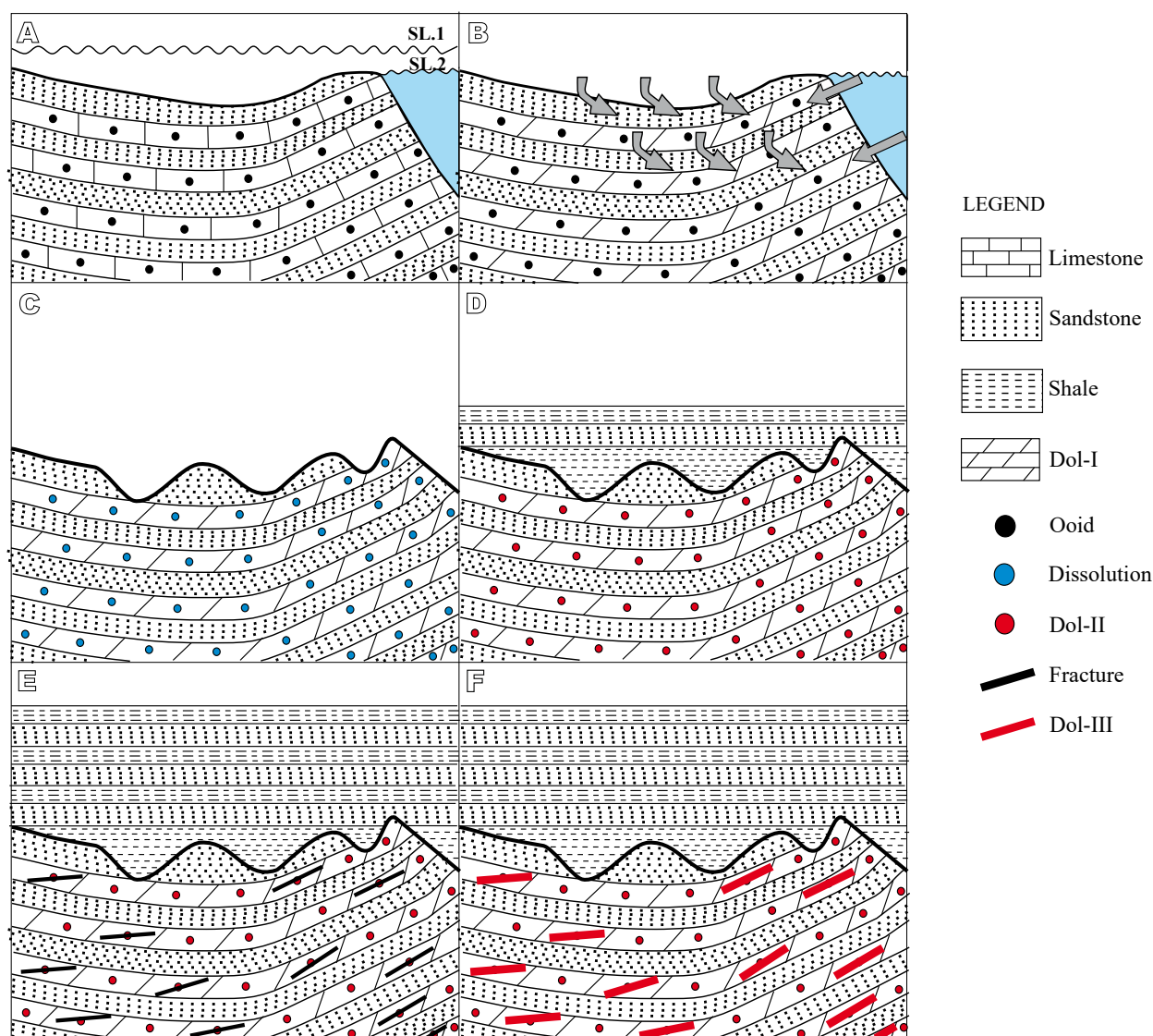
FIGURE 12. Conceptual model of dolomitization in the Cambrian Jutana Formation: A) Shale limestone-sandstone deposition in a tidal flat environment; B) Early Cambrian initial phase of dolomitization in the mixing-zone resulting in fine-crystalline dolomite (Dol. I); C) Selective dissolution of ooids in the partially dolomitized limestone during the Ordovician-Carboniferous exposure; D) Late Permian dolomite cementation (Dol. II) in the dissolved ooids; E) Fracture development related to post-orogenic event (post Eocene) and F) Fracture-filled coarse crystalline dolomite cementation (Dol. III) during post-orogenic uplift (i.e. post-Eocene) and activation of Salt Range thrust (i.e. Plio-Pleistocene).

An initial phase of dolomite (Dol. I) resulted from interaction with altered marine, Mg-rich fluids originated during earliest diagenetic phase, representing mixing-zone conditions during early Cambrian. This was followed by dissolution of the unaltered ooids by meteoric water during Ordovician-Carboniferous exposure (Dol. II and Dol. III). Dol. II and Dol. III are associated with burial conditions, where Dol. II formed in the earlier stage of burial (i.e. late Permian), whereas Dol. III formation was associated with burial and post-orogenic events before the activation of Salt Range Thrust (i.e. between Eocene and Plio-Pleistocene). Calcite precipitation and pyrite mineralization in the late stage mark the end of diagenetic history.

ACKNOWLEDGMENTS

REFERENCES

Ahmad, N., Ahsan, N., Sameeni, S.J., Mirag, M.A.F., Khan, B., 2013. Sedimentology of the Early-Middle Cambrian Jutana

Formation of Khewra Gorge area, Eastern Salt Range, District Chakwal, Pakistan. Science Inational Lahore, 25(3), 551-558.

Al-Aasm, I.S., 2000. Chemical and isotopic constraints for recrystallization of sedimentary dolomites from the Western Canada Sedimentary Basin. Aquatic geochemistry, 6, 227-248.

Allègre, C.J., Courtillot, V., Tapponnier, P., Hirn, A., Mattauer, M., Coulon, C., Jaeger, J.J., Achache, J., Schärer, U., Marcoux, J., Burg, J.P., Girardeau, J., Armijo, R., Gariépy, C., Göpel, C., Li, T., Xiao, X., Chang, C., Li, G., Lin, B., Teng, J., Wang, N., Chen, G., Han, T., Wang, X., Den, W., Sheng, H., Cao, Y., Zhou, J., Qiu, H., Bao, P., Wang, S., Wang, B., Zhou, Y., Ronghua, X., 1984. Structure and evolution of the Himalaya–Tibet orogenic belt. Nature, 307, 17-19.

Amorosi, A., 1997. Detecting compositional, spatial, and temporal attributes of glaucony: a tool for provenance research. Sedimentary Geology, 109, 135-153.

Bontognali, T.R.R., Vasconceles, C., Warthmann, R.J., Bernasconi, S.M., Durpraz, C., Stromenger, C.J., Mckanze, J.A., 2010. Dolomite formation with microbial mats in the coastal subkha of Abu Dhabi (UAE). Sedimentology, 57, 824-844.

Bowen, G.J., Daniels, A.L., Bowen, B.B., 2008. Paleoenvironmental isotope geochemistry and paragenesis of lacustrine and palustrine carbonates, Flagstaff Formation, Central Utah, U.S.A. Journal of Sedimentary Research, 78, 162-174.

Budd, D.A., 1997. Cenozoic dolomite of carbonate islands: their attributes and origin. Earth Science Reviewes, 42, 1-47.

Cantrell, D., Swart, P., Hagerty, R., 2004. Genesis and characterization of dolomite, Arab-D reservoir, Ghawar field, Saudi Arabia. Geo Arabia, 9(2), 1-26.

Chatterjee, S., Goswami, A., Christopher, R., 2013. The Longest Voyage: Tectonic, magmatic, and paleoclimatic evolution of the Indian Plate during its northward flight from Gondwana to Asia. Gondwana Research, 23, 238-267.

Dewit, J., Foubert, A., El Desouky, H.A., Muchez, P., Hunt, D., Vanhaecke, F., Swennen, R., 2014. Characteristics, genesis and parameters controlling the development of a large stratabound HTD body at Matienzo (Ramales Platform, Basque-Cantabrian Basin, Northern Spain). Marine and Petroleum Geology, 55, 6-25.

Dewit, J., Huysmans, M., Muchez, P., Hunt, D.W., Thurmond, J.B., Vergés, J., Saura, E., Fernandez, N., Romaire, I., Esestime, P., Swennen, R., 2012. Reservoir characteristics of fault-controlled hydrothermal dolomite bodies: Ramales Platform case study. In: Garland, J., Neilson, J.E., Laubach, S.E., Whidden, K.J. (eds.). Advances in Carbonate Exploration and Reservoir Analysis. Geological Society of London, 370 (Special Publications), 83-109.

Fleming, A., 1853. On the Salt Range in the Punjab. London, The Geological Society, 9, 189-200.

Fu, Q., Qing, H., Bergman, K.M., 2006. Dolomitization of Middle Devonian Winnipegosis carbonates in South-central Saskatchewan, Canada. Sedimentology, 53, 825-848.

Gansser, A., 1981. The geodynamic history of the Himalaya. In: Gupta, H.K., Delany, F.M. (eds.). Zagros, Hindu Kush, Himalaya: geodynamic evolution. Washington, American Geophysical Union (AGU), 111-121.

Gansser, A., 1964. Geology of Himalaya. New York, Interscience publishers, 289pp.

Gasparrini, M., Bechstadt, T., Boni, M., 2006. Massive hydrothermal dolomites in the southwestern Cantabrian Zone (Spain) and their relation to the late Variscan evolution. Journal of Marine and Petroleum Geology, 10, 1-26.

Geske, A., 2014. zur Erlangung des akademischen Grades eines Doktors der Naturwissenschaften an der Fakultät für Geowissenschaften der Ruhr-Universität Bochum. PhD Thesis. Ruhr-University Bochum, 241pp.

Geske, A., Goldstein, R.H., Mavromatis, V., Richter, D.K., Buhl, D., Kluge, T., John, C.M., Immenhauser, A., 2015. Magnesium isotope (δ^{26}) signatures of dolomites. Geochemica et Cosmochemica Acta, 149, 131-151.

Geske, A., Zorlu, J., Richter, D.K., Buhl. D., Niedermayr, A., Immenhauser, A., 2012. Impact of diagenesis and low-grade metamorphosis on isotopes ($\delta^{26}Mg$, $\delta^{13}C$, $\delta^{18}O$ and $^{87}Sr/^{86}Sr$) and elemental (Ca, Mg, Mn, Fe and Sr) signatures of Triassic sabkha dolomite. Chemical Geology, 332(333), 45-64.

Gee, E.R., 1945. The age of the saline series of the Punjab and of Kohat: India. National Academy of Sciences, Proceeding, Section B, 14(6), 269-310.

Ghauri, A.A.K., 1979. Sedimentary structures of the Jutana and baghanwala Formation Salt Range Pakistan. Geological Bulletin Universty of Peshawar, 12(13), 1-10.

Honarmand, J., Amini, A., 2012. Diagenetic processes and reservoir properties in the ooid grainstones of the Asmari Formation, Cheshmeh Khush Oil Field, SW Iran. Journal of Petroleum Science and Engineering, 81, 70-79.

Immenhauser, A., Buhl, D., Richter, D., Nieldermayr, A., Riechelmann, D., Dietzel, M., Schulte, U., 2010. Magnesium isotopes fractionation during low-Mg calcite precipitation in a limestone cave-Field study and experiments. Geochemica et Cosmochemica Acta, 74, 4346-4364.

Irwin, H., Curtis, C., Coleman, M., 1997. Isotope evidence of source of diagenetic carbonates formed during burial of organic-rich sediments. Nature, 269, 209-213.

Jaffres, J.B.D, Shields, G.A., Wallmen, K., 2007. The Oxygen isotope evolution of sea water: A critical review of a long-standing controversy and an improved geological water cycle model for the last 3.4 billion years. Earth-Science Reviews, 83, 83-122.

Jones, G.D., Whitaker, F.F., Smart, P.L., Sanford, W.E., 2002. Fate of reflux brines in carbonate platforms. Geology, 30, 371-374.

Kadri, I.B., 1995. Petroleum Geology of Pakistan. In: Kadri, I.B. (ed.) Petroleum Geology of Pakistan. Karachi, Pakistan Petroleum Ltd., 1-300.

Kazmi, A.H., Jan, M.Q., 1997. Geology and tectonics of Pakistan. Karachi (Pakistan), Graphic Publishers, 545pp.

Keith, B.D., 1989. Reservoirs resulting from facies-independent dolomitization: Case histories from the Trenton and Black

River carbonate rocks of the Great Lakes Area. In: Keith, B.D. (ed.). The Trenton Group (Upper Ordovician Series) of Eastern North America. American Association of Petroleum Geologists, Studies in Geology, 29, 267-276.

Khan, M.A., Khan, M.J., 1977. Stratigraphy and petrography of the Jutana Dolomite, Khewra Gorge Khewra, Jehlum District; Punjab: Pakistan. Geological Bulletin University of Peshawar, 9(10), 43-66.

Last, L.S., 1990. Lacustrine dolomite-An overview of modern, Holocene and Pleistocene occurrences. Earth-Science Reviews, 27, 221-263.

Lillie, R.J., Johnson, G.D., Yousuf, M.H., Zamin, A.S, Yeats, R.S., 1987. Structural development within the Himalayan foreland fold and thrust belt of Pakistan. In: Beaumont, C., Tankard, A.J. (eds.). Sedimentary basins and basin forming mechanisms. Canadian Society of Petroleum Geologists, 379-392.

Machel, H.G., 2004. Concepts and models of dolomitisation: a critical reappraisal. In: Braithwaite, C.J.R., Rizzi, G., Darke, G. (eds.). The geometry and petrogenesis of dolomite hydrocarbon reservoir. The Geological Society of London, 235 (Special Publications), 7-63.

Machel, H.G., Lonnee, C.J., 2002. Hydrothermal dolomite-A product of poor definition and imagination. Sedimentary Geology, 152, 163-171.

Machel, H.G., Krouse, H.R., Sassen, R., 1995. Products and distinguishing criteria of bacterial and thermochemical sulfate reduction. Applied Geochemistry, 10, 373-389.

Malinconico, L.L., 1989. Crustal thickness estimates for the western Himalaya. In: Malinconico, L.L., Lillie, R.J. (eds.). Tectonics of the Western Himalayas. Geological Society of America, 232 (Special paper), 237-242.

Martín-Martín, J.D., Gomez-Rivas, E., Bover-Arnal, T., Travé, A., Salas, R., Moreno-Bedmar, J.A., Tomás, S., Corbella, M., Teixell, A., Vergés, J., Stafford, S.L., 2013. The upper Aptian-lower Albian syn-rift carbonate succession of the southern Maestrat Basin (Spain): Facies architecture and fault-controlled strata-bound dolostones. Cretaceous Research, 41, 217-236.

Mazullo, S.J., 1977. Shrunken (geopetal) ooids: Evidence of origin unrelated to evaporite diagenesis. Sedimentary petrology, 47(1), 392-397.

McRae, S.G., 1972. Glauconite. Earth-Science Reviews, 8(4), 397-440.

Melim, L.A., Scholle, P.A., 2002. Dolomitization of the Capitan Formation forereef facies (Permian, west Texas and New Mexico): seepage reflux revisited. Sedimentology, 49, 1207-1227.

Molnar, P., Tapponnier, P., 1977. The collision between India and Asia. Scientific American, 236(4), 30-41.

Müller, D.W., McKenzie, J.A., Mueller, P.A., 1990. Abu Dhabi sabkha, Persian Gulf, revisited: Application of strontium isotopes to test an early dolomitization model. Geology, 18, 618-621.

Nader, F.H., Swennen, R., 2004. The hydrocarbon potential of Lebanon: New insights from regional correlations and studies of Jurassic dolomitization. Journal of Petroleum Geology, 27, 253-275.

Nader, F.H., Swennen, R., Ellam, R., 2007. Field geometry, petrography and geochemistry of a dolomitisation front (Late Jurassic, central Lebanon). Sedimentology, 54, 1093-1119.

Nader, F.H., Swennen, R., Ellam, R., 2004. Reflux stratabound dolostone and hydrothermal volcanism-associated dolostone: a two-stage dolomitization model (Jurassic, Lebanon). Sedimentology, 51, 339-360.Noetling, P., 1901. Beitragezur Geologieder Salt Range, insbesondereder permichenund triasuchen Ablagerungen: Ueues Jahrb. Miner Beilage Band, 14, 369-471.

Odin, G.S., Matter, A., 1981. De glauconiarum origine. Sedimentology, 28, 611-641.

Patterson, R.J., Kinsman, D.J.J., 1981. Hydrologic framework of a sabkhas along the Arabian Gulf. American Association of Petroleum Geologists (AAPG), 65, 1457-1475.

Prokoph, A., Shields, G.A., Veizer, J., 2008. Compilation and time series analysis of a marine carbonate $\delta^{18}O$, $\delta^{13}C$, $^{87}Sr/^{86}Sr$ and $\delta^{34}S$ data base through earth history. Earth-Science Reviews, 87, 113-133.

Qing, H., Bosence, D.W.J., Rose, E.P.F., 2001. Dolomitization by penesaline sea water in Early Jurassic peritidal platform carbonates, Gibraltar, western Mediterranean. Sedimentology, 48, 153-163.

Quadri, V.N., Quadri, S.M.G.J., 1996. Anatomy of success in oil and gas exploration in Pakistan. Oil and Gas Journal (OGJ), 13, 92-97.

Radke, B.M., Mathis, R.L., 1980. On the formation and occurrence of saddle dolomites. Journal of Sedimentary Research, 50(4), 1149-1168.

Seeber, L., Armbruster, J.G., 1979. Seismicity in the Hazara arc in northern Pakistan: décollement versus basement faulting. In: Farah, A., De Jong, K. (eds.). Geodynamics of Pakistan. Quetta, Geological Survey of Pakistan (GSP), 131-142.

Sellwood, B.W., Beckett, D., 1991. Ooid microfabrics: the origin and distribution of high intra-ooid porosity; Mid-Jurassic reservoirs, S. England. Sedimentary Geology, 71, 189-193.

Shah, S.M.I., 2009. Stratigraphy of Pakistan, Geological Survey of Pakistan, Memoir 22, 381pp.

Shah, M.M., Khan, S., Toqeer, M., Unpublished. Fluid flow evolution resulted in multiphase dolomitization in the Jutana Formation (Cambrian), Salt Range and adjoining areas, NW Pakistan: Evidences from mineralogical analysis, geochemical studies and isotopic signatures. Sedimentary Geology. [Accepted]

Shah, M.M., Nader, F. H., Garcia, D., Swennen, R., Ellam, R., 2012. Hydrothermal Dolomites in the Early Albian (Cretaceous) Platform Carbonates (NW Spain): Nature and Origin of Dolomites and Dolomitising Fluids. Oil & Gas Science and Technology, IFP Energies nouvelles, 67(1): 97-122.

Shah, M.M., Nader, F.H., Dewit, J., Swennen, R., Garcia, D., 2010. Fault-related hydrothermal dolomites in Cretaceous carbonates (Cantabria, northern Spain): Results of

petrographic, geochemical and petrophysical studies. Bulletin de la Société Géologique de France, 181(49), 391-407.

Sibley, D.F., Gregg, J.M., 1987. Classification of dolomite rock textures. Journal of Sedimentary Petrology, 57, 967-975.

Swennen, R., Dewit, J., Fierens, E., Muchez, P., Shah, M., Nader, F.H., Hunt, D., 2012. Multiple dolomitisation events along the Pozalagua Fault (Pozalagua Quarry, Basque-Cantabrian Basin, Northern Spain). Sedimentology, 59, 1345-1374.

Teichert, C., 1964. Recent German work on the Cambrian and Saline Series of the Salt Range, west Pakistan. Geological Survey of Pakistan, Records, 11(1), 20pp.

Veizer, J., Ala, D., Azmy, K., Bruckschen, P., Buhl, D., 1999. $^{87}Sr/^{86}Sr$, $\delta^{13}C$ and $\delta^{18}O$ evolution of Phanerozoic sea water. Journal of Chemical Geology, 161, 59-88.

Wandrey, C.J., Law, B.E., Shah, H.A., 2004. Patala-Nammal composite total petroleum system, Kohat-Potwar geological province, Pakistan. U.S. Geological Survey Bulletin 2208-B, 20pp.

Warren, J., 2000. Dolomite: occurrences, evolution and economically important associations. Earth-Science Reviews, 52, 1-81.

Yeats, S.R., Hussain, A., 1987. Timing of structural events in the Himalayan foothills of north-western Pakistan. Geological Society of America, Bulletin, 99, 161-175.

Yeats, R.S, Lawrence, R.D., 1984. Tectonics of the Himalayan thrust belt in northern Pakistan. In: Haq, B.U., Milliman, J.D. (eds.). Marine geology and oceanography of Arabian Sea and Coastal Pakistan. New York, Von Nostrand Reinhold, 177-198.

Yeats, R.S, Khan, S.H., Akhtar, M., 1984. Late Quaternary deformation of the Salt Range of Pakistan. Geological Society of America, Bulletin, 95(8), 958-966.

Zenger, D.H., Dunham, J.B., Ethington, R.L., 1980. Concepts and models of dolomitization. Society for Sedimentary Geology (SEPM), 28 (Special Publication), 320pp.

Zhang, F., Xu, H., Kornishi, H., Shelobolina, E.S., Roden, E.E., 2012. Polysaccharide-catalyzed nucleation and growth of disordered dolomite: A potential precursor of sedimentary dolomite. American Mineralogist, 97, 556-567.